Supporting Information

Novel Ln^{3+}/Al^{3+} metallacrown multifunctional material for latent fingerprints detection, luminescent thermometer and luminescent sensor

Han Yan,[a] Claudia M. S. Calado,[b] Hao Wang,[a] Muralee Murugesu*[b] and Wen-Bin Sun*[a]

[a] *Key Laboratory of Functional Inorganic Material Chemistry Ministry of Education, School of Chemistry and Material Science Heilongjiang University, 74 Xuefu Road, Harbin 150080, P. R. China.*

E-mail: wenbinsun@126.com

[b] *Department of Chemistry and Biomolecular Sciences, University of Ottawa, Ottawa, Ontario K1N 6N5, Canada*

E-mail: m.murugesu@uottawa.ca

1. Experimental section

Preparation of $[LnAl_4(shi)_4(C_7H_5O_3)_4Na(H_2O)_5]\cdot 0.5(H_2O)\cdot 4DMF$ (LnMC)

Taking DyMC as an example, aluminum nitrate (1 mmol, 0.3751 g) was dissolved in 10 mL of DMF to configure a colorless and transparent aluminum nitrate solution and set aside. In a 50 mL flask, $Dy(NO_3)_3\cdot 6H_2O$ (0.25 mmol, 0.1142 g), salicylhydroxamic acid (H_3shi) (1 mmol, 0.1531 g), and sodium p-hydroxybenzoate (4 mmol, 0.6404 g) were mixed in 10 mL of DMF to obtain an opaque white suspension. Aluminum nitrate solution was slowly added to the suspension and the turbidity gradually disappeared, resulting in a slightly pinkish transparent solution. The solution was stirred continuously for 12 hours and subsequently filtered to obtain a pale-yellow filtrate, which was slowly evaporated at room temperature. After 15 days, crystals suitable for X-ray analysis were collected. Yield: 17%. Elemental analysis calcd (%) for $C_{68}H_{75}Al_4DyN_8NaO_{33.5}$: C 44.54, H 4.12, N 6.11; found: C 44.49, H 4.06, N: 6.15. The synthesis of other crystals follows the same procedure, using $Ln(NO_3)_3\cdot 6H_2O$ (Ln = Sm, Eu, Tb, Gd, Ho, Er, Yb).

Preparation of $[Tb_{1-x}Sm_xAl_4(shi)_4(C_7H_5O_3)_4Na(H_2O)_5]\cdot 0.5(H_2O)\cdot 4DMF$ ($Tb_{1-x}Sm_xMC$)

The $Tb_{1-x}Sm_xMC$ (x = 0, 0.1, 0.3, 0.5, 0.7, 0.9, 1.0) were synthesized similarly to DyMC except for the use of a mixture of $Tb(NO_3)_3\cdot 6H_2O$ and $Sm(NO_3)_3\cdot 6H_2O$.

Preparation of PMMA/LnMC films

The polymethyl methacrylate (PMMA) (0.1 g) was dissolved in DMF (8 mL) and stirred at room temperature for 15 min. Solutions of complexes LnMC (Ln = Tb^{3+} or Sm^{3+}) (0.01 g) were prepared by dissolving in 2 mL DMF and then added dropwise to the solution of PMMA. After two hours of stirring, the solution was transferred to a glass plate and a heating plate at 70 ℃ was used to evaporate DMF and form clear films.

Materials and Characterization

All raw materials and solvents were purchased commercially and used without further purification. Elemental analyses (C, H and N) were conducted using a PerkinElmer 2400 analyzer. Fourier-transform infrared (FTIR) spectroscopy was performed with a Perkin Elmer 100 spectrophotometer, measuring in the range of 4000-500 cm^{-1} using spectroscopic grade potassium bromide (KBr) and the pellet method. Powder X-ray diffraction (PXRD) patterns were obtained on a Rigaku D/Max-3B X instrument within a range of 5-50° at room temperature. Thermogravimetric analyses (TGA) were carried out on a PerkinElmer STA 6000 from 30-800 °C. Ultraviolet (UV) spectra were collected using a PerkinElmer LAMBDA 35 spectrometer at room temperature. Excitation and emission spectra were recorded using a Perkin Elmer FL6500 luminescence spectrophotometer. All the digital photographs were taken under 254 nm UV light. Crystal data were collected on a Nonius Kappa CCD diffractometer with Mo Kα radiation (λ = 0.71073 Å). The structures of the complexes were solved by direct methods and refined on F^2 by full-matrix least-squares using the SHELXTL[1] and Olex 2[2] programs. All non-hydrogen atoms were refined with isotropic displacement parameters. Detailed crystallographic data for the complexes are summarized in Table S1, and selected bond lengths and angles for complexes are listed in Table S2.

2. Additional figures and tables

Table S1. Crystallographic data for **DyMC**.

Complex	**DyMC**
Empirical formula	$C_{136}H_{150}Al_8Dy_2N_{16}Na_2O_{67}$
FW ($g.mol^{-1}$)	3667.53
Crystal system	tetragonal

Space group	P4nc
Temperature (K)	293
a (Å)	17.1664(7)
b (Å)	17.1664(7)
c (Å)	15.3325(17)
α (°)	90
β (°)	90
γ (°)	90
V (Å^3)	4518.3(6)
ρ_{calcd} (g.m^{-3})	1.348
μ (mm^{-1})	0.952
F(000)	1872.0
Independent relections	4327
R_{int}	0.0328
R_1 [I > 2σ(I)]	0.0526
wR_2 (all data)	0.1531
Goodness of fit on F^2	1.115
CCDC numbers	2377154

Table S2. Selected bond lengths (Å) and angles (°) for **DyMC**.

Dy1-Na1	3.434(10)	Dy1-O6^{3}	2.364(6)
Dy1-O4^{1}	2.311(7)	Dy1- O6^{1}	2.364(6)
Dy1- O4^{2}	2.311(7)	Dy1- O6^{2}	2.364(6)
Dy1- O4^{3}	2.311(7)	Dy1- O6	2.364(6)
Dy1- O4	2.311(7)		
O4^{1}-Dy1-Na1	118.9(2)	O4^{1}-Dy1- O6	145.0(2)
O4^{2}-Dy1 Na1	118.9(2)	O4^{2}-Dy1- O6^{3}	145.0(2)
O4-Dy1- Na1	118.9(2)	O4^{1}-Dy1- O6^{2}	138.4(2)
O4^{3}-Dy1- Na1	118.9(2)	O4^{3}-Dy1- O6^{1}	138.4(2)
O4^{3}-Dy1- O4^{1}	76.51(19)	O4-Dy1- O6^{1}	145.0(2)
O4^{1}-Dy1- O4^{2}	76.52(19)	O4^{3}-Dy1- O6^{3}	78.6(2)
O4^{2}-Dy1- O4	76.52(19)	O4-Dy1- O6	78.6(2)
O4^{3}-Dy1- O4	76.51(19)	O4^{2}-Dy1- O6^{2}	78.6(2)
O4^{1}-Dy1- O4	122.3(4)	O6^{2}-Dy1- Na1	49.93(16)
O4^{3}-Dy1- O4^{2}	122.3(4)	O6-Dy1- Na1	49.93(16)
O4-Dy1- O6^{3}	138.4(2)	O6^{1}-Dy1- Na1	49.93(17)
O4^{1}-Dy1- O6^{3}	82.8(3)	O6^{3}-Dy1- Na1	49.93(16)
O4^{2}-Dy1- O6	138.4(2)	O6-Dy1- O6^{1}	99.9(3)
O4-Dy1- O6^{2}	82.8(3)	O6-Dy1- O6^{2}	65.52(18)
O4^{2}-Dy1- O6^{1}	82.8(3)	O6^{1}-Dy1- O6^{2}	65.52(18)
O4^{3}-Dy1- O6^{2}	145.0(2)	O6^{1}-Dy1- O6^{3}	65.52(18)
O4^{3}-Dy1- O6	82.7(3)	O6-Dy1- O6^{3}	65.52(18)
O4^{1}-Dy1- O6^{1}	78.6(2)	O6^{2}-Dy1- O6^{3}	99.9(3)

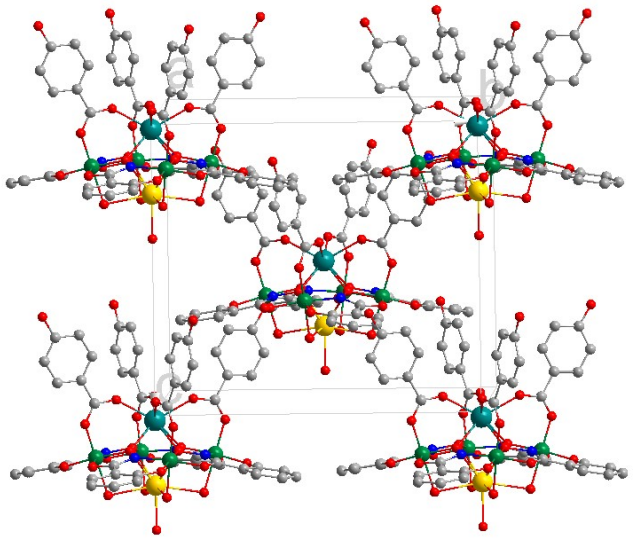

Fig. S1. The packing diagram of **DyMC**. H atoms and solvent are omitted for clarity. Colour code: Dy (teal), Al (green), O (red), N (blue), C (grey), Na (yellow).

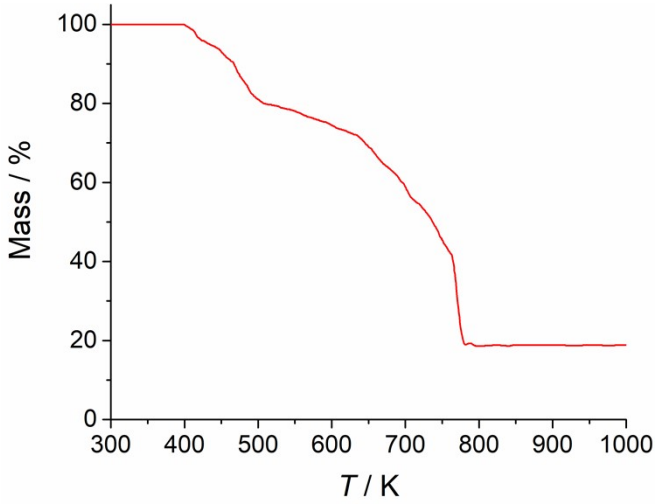

Fig. S2. Thermogravimetric analysis of **DyMC**.

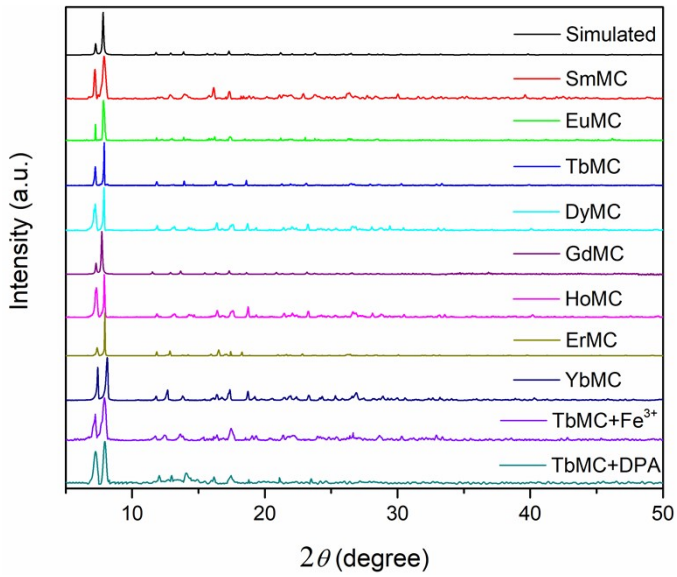

Fig. S3. Experimental and simulated powder X-ray diffraction (PXRD) patterns.

Table S3. Continuous Shape Measures (CShMs) of the coordination geometry for Dy^{3+} ion in **DyMC** (S values calculated with the Shape program). The *S* values indicated the proximity to the ideal polyhedron, thus, an $S = 0$ corresponds to the non-distorted polyhedron. The three closer ideal geometries to the real complexes are listed.

	CShM			CShM value
Dy^{3+}	OP-8	D_{8h}	Octagon	32.434
	HPY-8	C_{7v}	Heptagonal pyramid	23.545
	HBPY-8	D_{6h}	Hexagonal bipyramid	16.172
	CU-8	O_h	Cube	8.491
	SAPR-8	D_{4d}	Square antiprism	0.832
	TDD-8	D_{2d}	Triangular dodecahedron	2.585
	JGBF-8	D_{2d}	Johnson gyrobifastigium J26	17.314
	JETBPY-8	D_{3h}	Johnson elongated triangular bipyramid J14	30.511
	JBTPR-8	C_{2v}	Biaugmented trigonal prism J50	3.214
	BTPR-8	C_{2v}	Biaugmented trigonal prism	2.062
	JSD-8	D_{2d}	Snub diphenoid J84	5.988
	TT-8	T_d	Triakis tetrahedron	9.363
	ETBPY-8	D_{3h}	Elongated trigonal bipyramid	25.674

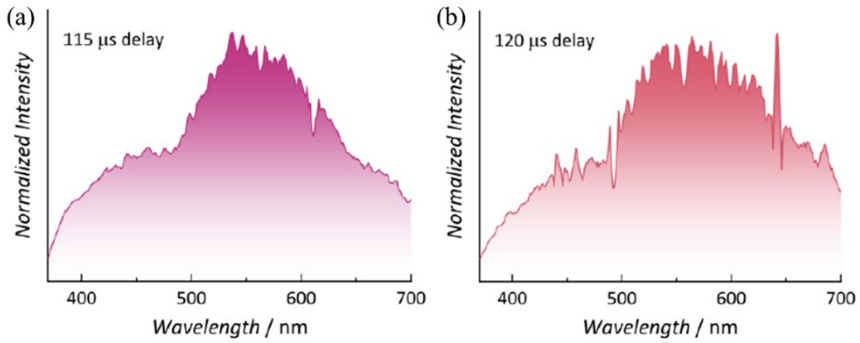

Fig. S4. Time-resolved emission spectra applying a delay of (a) 115 µs and (b) 120 µs after excitation (λexc = 283 nm) of **GdMC**, obtained at 77 K.

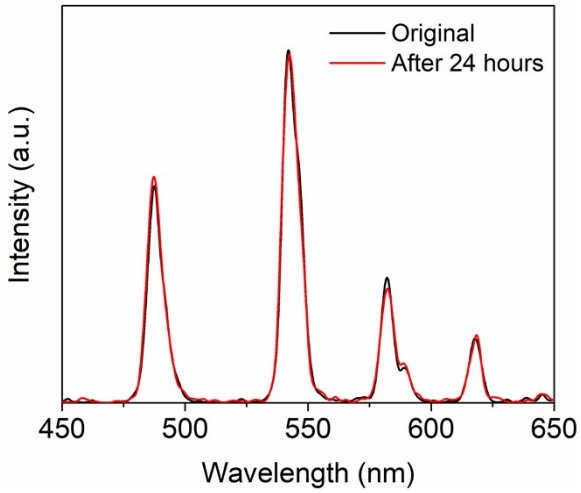

Fig. S5. Emission spectra of **TbMC** in ethanol solution.

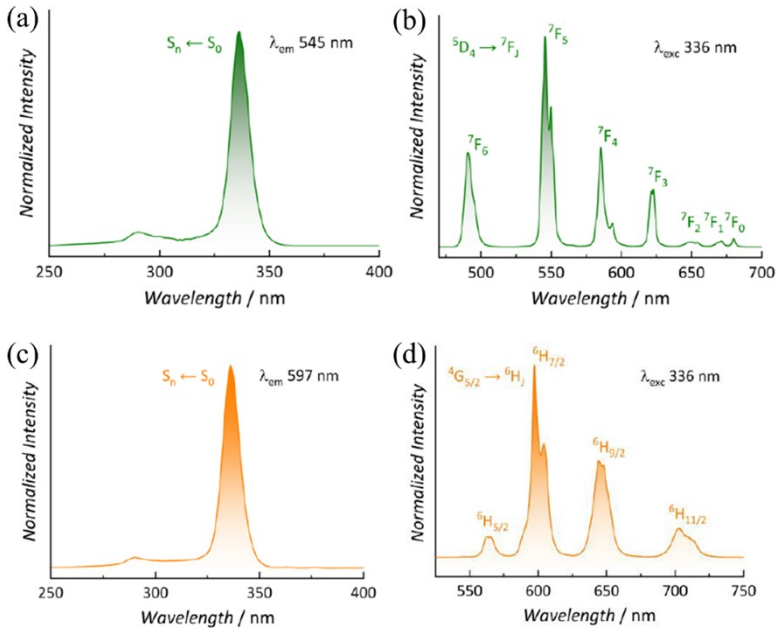

Fig. S6. (a) Excitation and (b) emission spectra of **TbMC**. (c) Excitation and (d) emission spectra of **SmMC** collected at 20 °C.

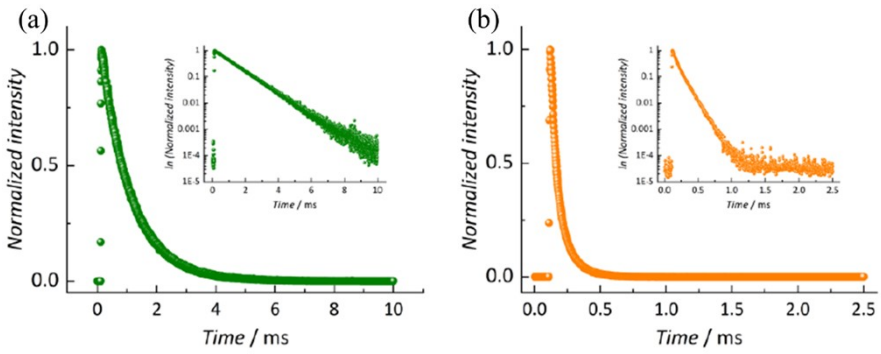

Fig. S7. Emission decay curves of (a) **TbMC** (λem = 545 nm) and (b) **SmMC** (λem = 597 nm), and linearization of decay curves (inserts), obtained at 20 °C. λexc = 336 nm.

Table S4. Lifetime values obtained from the fitting of decay curves of **TbMC** and **SmMC**.

Temperature	τ_{Tb} / μs	τ_{Sm} / μs
5 °C	1220	71
10 °C	1151	70
15 °C	1083	70
20 °C	1011	69
25 °C	944	69
30 °C	868	68
35 °C	788	68
40 °C	710	67
45 °C	635	66
50 °C	570	65
55 °C	506	64
60 °C	447	64

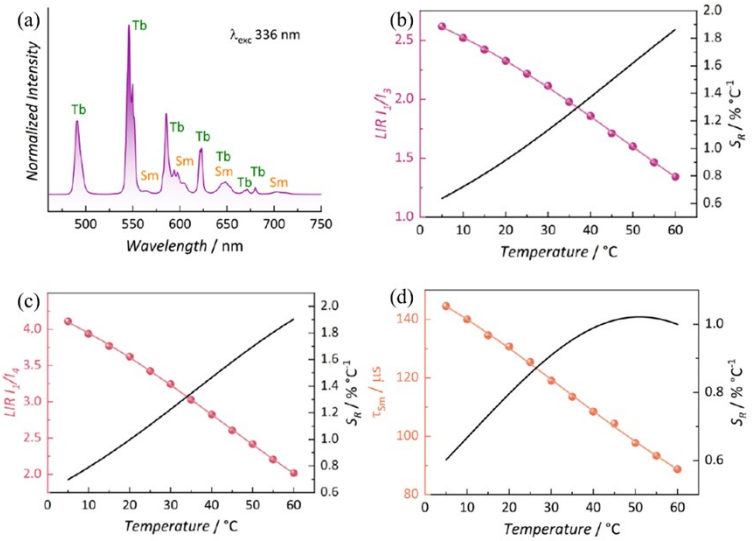

Fig. S8. (a) Varying-temperature emission spectra of **$Tb_{0.1}Sm_{0.9}$MC**. λexc = 336 nm. The areas selected for LIR are highlighted in gray. (b) Temperature dependence of LIR (pink) and its fitting with a Boltzmann-like function (best-

fitting parameters: $A_1 = 3.26$, $A_2 = 0.02$, $x_0 = 48.23$, $r^2 = 0.999$), and relative thermal sensitivity of LIR (black) using I_1/I_3 as thermometric parameter. (c) Temperature dependence of LIR (salmon) and its fitting with a Boltzmann-like function (best-fitting parameters: $A_1 = 5.20$, $A_2 = 0.20$, $x_0 = 42.94$, $r^2 = 0.999$), and relative thermal sensitivity of LIR (black) using I_1/I_4 as thermometric parameter. (d) Temperature dependence of τ_{Sm} (orange) and its fitting with a Boltzmann-like function (best-fitting parameters: $A_1 = 0.18$, $A_2 = 0.05$, $x_0 = 33.12$, $r^2 = 0.999$) and relative thermal sensitivity of thermometric parameter (black).

Table S5. Lifetime values obtained from the fitting of decay curves of **$Tb_{0.1}Sm_{0.9}$MC**.

Temperature	τ_{Tb} / μs	$\langle\tau_{Sm}\rangle$/ μs
5 ℃	1221	145
10 ℃	1152	140
15 ℃	1082	134
20 ℃	1010	131
25 ℃	938	125
30 ℃	861	119
35 ℃	783	113
40 ℃	707	108
45 ℃	634	104
50 ℃	564	98
55 ℃	501	93
60 ℃	442	89

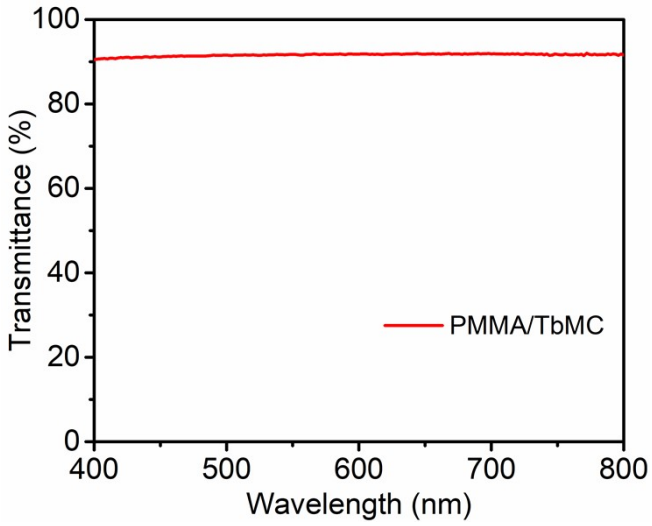

Fig. S9. UV transmittance of **PMMA/TbMC**.

3. References

1. G. M. Sheldrick, *Acta Crystallogr., Sect. A: Found. Adv.*, 2008, 64, 112-122.
2. O. V. Dolomanov, L. J. Bourhis, R. J. Gildea, J. A. K. Howard and H. Puschmann, *J. Appl. Crystallogr.*, 2009, 42, 339-341.